Int. J. Renew. Energy Dev. 2023, 12 (6), 1018-1029


Contents list available at IJRED website

**International Journal of Renewable Energy Development**

Journal homepage: https://ijred.undip.ac.id

**Research Article**

# Effect of the non-uniform combustion core shape on the biochar production characteristics of the household biomass gasifier stove

Somchet Chaiyalap[a], Ritthikrai Chai-ngam[a], Juthaporn Saengprajak[b], Jenjira Piamdee[a], Apipong Putkham[c], Arnusorn Saengprajak [a*]

[a] *Department of Physics, Faculty of Science, Mahasarakham University, Mahasarakham, 44150, Thailand*

[b] *Department of Biology, Faculty of Science, Mahasarakham University, Mahasarakham, 44150, Thailand*

[c] *Faculty of Environment and Resource Studies, Mahasarakham University, 44150, Thailand*

**Abstract**. The global demand for biochar in agricultural and carbon sequestration applications is increasing; nevertheless, biochar production using the 50-liter household biomass gasifier stove (50L-HBGS) in Thailand found major issues that need to be improved. The objective of this study was to study the effects of the airflow in the non-uniform combustion core shape (NCCS) on the biochar production characteristic of the 50L-HBGS. The new design of the NCCS was constructed and studied to replace the existing combustion core shape (ECCS) at Mahasarakham University. The height, air inlet, and air outlet diameters of the NCCS were designed at 45, 24, and 11.4 cm, respectively. The NCCS with 21 holes of the pyrolysis gas outlet, a diameter of 4 mm for each, was integrated into the 50L-HBGS and performed comparative tests to the ECCS using 9 kg of bamboo wood chunks in three consecutive experiments. The airflow and the combustion behavior were studied through the stove temperature profiles, which were recorded every 5 minutes using a digital data logger. The biochar products were studied using the scanning electron microscope (SEM) with the energy dispersive x-ray spectroscopy (EDS), Fourier transform infrared spectroscopy (FTIR), and the proximate analysis technique. The study indicated that the 50L-HBGS with the NCCS made significantly improved the airflow rates in the combustion core, resulting in better continuous burning during the ignition state than with the ECCS. Moreover, the pyrolysis temperatures were significantly improved, it was provided temperatures during the pyrolysis process reached higher than 500 °C, resulting in the liquid tar being removed and no unburned wood chunks remaining at the end. The characterization result demonstrated that the 50L-HBGS with the NCCS had created biochar within a range of micropore and macrospore sizes and high fixed carbon content, which could be advantageously used for different agricultural and carbon sequestration applications.

**Keywords:** Biochar, Pyrolysis, Bamboo, Gasifier Stove, Heat Transfer


Received: 15th July 2023; Revised: 30th August 2023; Accepted: 12th Sept 2023; Available online: 23rd Sept 2023

## 1. Introduction

With the world moving toward carbon neutrality, biochar application is expanding beyond uses in agriculture and home heating (Nair *et al.*, 2023; Kurniawan *et al.*, 2023). Biochar also has potential usage as an adsorption material for carbon sequestration techniques (Gou *et al.*, 2022; Rustamaji *et al.*, 2022; Abdullha *et al.*, 2023). According to Elkhlifi *et al.* (2023) and Qian *et al.* (2023), biochar is intentionally thermal converted organic material that is added to soil to enhance soil characteristics and increase carbon storage over the long term. Biochar can be produced from several sources of organic material feedstock, such as food waste, agricultural waste, macroalgae, etc. (Idris *et al.*, 2021; Ibitoye *et al.*, 2022; Chen *et al.*, 2022), with variant techniques, for instance, pyrolysis, gasification, torrefaction, hydrothermal carbonization, etc. (Gabhane *et al.*, 2020; Chen *et al.*, 2020; Onokwai *et al.*, 2022). However, the biochar converting method is commonly classified into two main methods, i.e., hydrothermal carbonization method and pyrolysis method (Liu *et al.*, 2021). Whereas hydrothermally carbonization is suitable for moist feedstocks, pyrolysis is best for dry biomass (You *et al.*, 2023; Chen *et al.*, 2023). Even though pyrolysis is more complicated in production with the temperature range of 300-700 °C or above, and the process is gone under oxygen-limited conditions (Tomczyk *et al.*, 2020), it provides biochar with a higher surface area, larger pore size, lower toxicity and more stable (high carbon-rich) than hydrothermal technique (Jian *et al.*, 2018; Liu *et al.*, 2021) which benefit for soil treatment and application as adsorption material (Muzyka *et al.*, 2023; Kkaledi *et al.*, 2023). The slow pyrolysis in the range of 350-600 °C is produces more biochar, while at temperatures higher than 700 °C (fast pyrolysis), the yield of the liquid and gas fuel is increased (Panyoyai *et al.*, 2019; Petchaihan *et al.*, 2020; Gabhane *et al.*, 2020). At the commodity level, small pyrolysis stoves, such as the Anila stove, are popularly used to convert feedstocks into biochar (Pradana & Prasetya, 2017). The Anila stove has a couple with a small inner cylinder as the combustion core and a larger outer cylinder, a pyrolysis section, with tiny holes connecting the two sections. The stove can produce both heat for domestic cooking and biochar as a byproduct, with low emission dissipation (Smebye *et al.*, 2017; Zahida *et al.*, 2017), and has a $CO_2$ sequestration ability of over 2,500 kg per year by estimates (Pradana & Prasetya, 2017). The

* Corresponding author
Email: Email: arnusorn.s@msu.ac.th (A. Saengprajak)

https://doi.org/10.14710/ijred.2023.56575
ISSN: 2252-4940/© 2023.The Author(s). Published by CBIORE

Anila stove has been widely used on a household scale in India and Southeast Asia (Boateng *et al.*, 2015; Carter & Shackley, 2011). Recently in Thailand, although the number of people using the 50L-HBGS (modified Anila stove) has increased, users always claim that it still has problems with stove production characteristics, which reflects the productivity of biochar (Maneekhat & Khamdaeng, 2022; Srisophon *et al.*, 2020). The stove production characteristic problems concern; non-continuous burning (Sittioad *et al.*, 2022), needing more tendering during operation, and remaining tar and unburned biomass at the end, which is a similar problem to the Anila stove in Africa (Mosisa *et al.*, 2019) that needs to be improved.

Recently, the development of the 50L-HBGS has focused on the appropriated combustion core puncher sizes, numbers, and bore positions in the core with the variant sizes of stoves and feedstocks (Petchaihan *et al.*, 2020; Maneekhat & Khamdaeng, 2022; Srisophon *et al.*, 2020; Panyoyai *et al.*, 2019; Intagun *et al.*, 2018). Even if previous studies revealed the relation of core puncher sizes and positions to the temperature distributions in biochar productions, however, no further method information points out methods for solving problems as stated above.

Since the studies only used the straight combustion core shape in the 50L-HBGS, the current research still lacks available information options of other combustion core types, which would be moderated by the problems above. Therefore, this research proposes to study application of the NCCS to the 50L-HBGS, which would be provide higher airflow rates, result in better continuous burning, higher pyrolysis temperatures, and better quality of biochar products.

For the reasons above, this research aims to improve airflow in the combustion core of the 50L-HBGS by using the non-uniform combustion core shape (NCCS) to replace the existing combustion core shape (ECCS), the most found combustion core type in the local market. The comparative test of both cases in the burning behaviors, pyrolysis processing temperatures, and quality of biochar products was done by using the ANOVA statistical technique, Fourier transform infrared spectroscopy (FT-IR), scanning electron microscopy (SEM), and the proximate analysis technique in order to indicate the improvement of the biochar production characteristics by the 50L-HBGS.

## 2. Materials and Methods

### *2.1 Design of the NCCS*

In order to make the 50L-HBGS user-friendly and to achieve higher biochar qualities, the NCCS in the 50-L HBGS was designed to increase the volume of the air inlet and the total heat transfer area, which should result in sufficient airflow for continuing combustion in the core. Also, it must be provided that the bottom stove's temperature reaches 500 °C, which is the optimum temperature for biochar production (Li *et al.*, 2023; Ippolito *et al.*, 2020) and sufficient to remove volatile matter and develop more pore structure (Balmuk *et al.*, 2023; Basinas *et al*, 2023). Therefore, the new combustion core, the NCCS (Figure 1b) was made as a non-uniform tube, which had a larger air inlet diameter and a smaller air outlet diameter (number 2 in Figure 1c). It was made of an iron tube with a thickness of 4 mm and a height of 45 cm. The diameter of the air inlet section is 24 cm and then slopes downward to the same size as the air outlet section, which is 11.4 cm (number 3 in Figure 1c) at a length of 15 cm from the bottom of the core. It was bored with 21 points of 4 mm core puncture diameter. With this design, the overall volume of the core is 0.0098 $m^3$, an increase of 114% compared to the ECCS. Furthermore, the overall surface area of the NCCS had expanded by 103.5% to 0.328 $m^2$ compared to the ECCS.

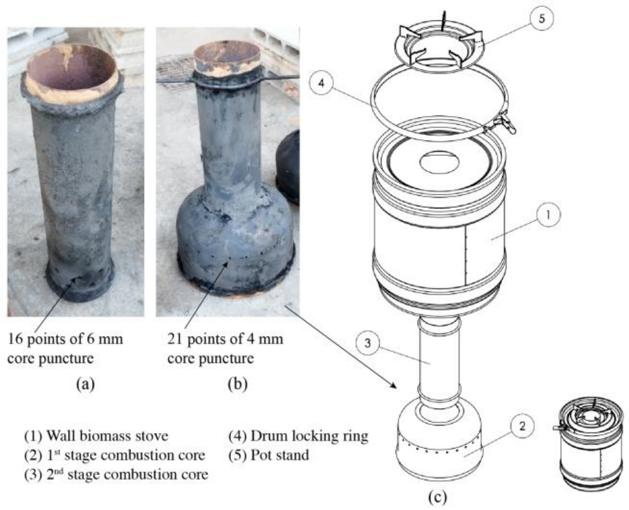


**Fig. 1** The combustion core of the 50L-HBGS; (a) the existing combustion core shape (ECCS) (b) the non-uniform combustion core shape (NCCS) (c) components of the 50L HBG with the NCCS

The ECCS was made of a straight iron tube 4 mm in thick, had a bottom bore with 16 points of 6 mm core puncture diameter (Figure 1a), was 45 cm high, and had an outer diameter of 11.4 cm. The outer walls of both cases were covered by ceramic sheet insulation. The NCCS and the ECCS were integrated into the 50L-HBGS and performed comparative experiments on the biochar production performance.

### *2.2 Stove Performance Analysis*

In general cooking stoves, the water boiling test is applied to test the performance of the stoves. As indicated in the standard water boiling test (Chen *et al.*, 2023; Ajieh *et al.*, 2023), the stove process must be stopped after the water boiling. Since the 50L-HBGS process is different from a general combustion stove, it can not stop the stove process after water boiling. Therefore, the water boiling test was not applicable to this study. And, because the 50L-HBGS can produce both biochar and pyrolysis gas, the percent yield of biochar (%BC) and the percent of produced gas (%PG) were used to compare the difference of stove performance when using the NCCS and the ECCS. The following equation was used to determine biochar's yield from the stove.

$$\%BC = \frac{W_{BC}}{W_{IB} - W_{NC}} \times 100 \quad (1)$$

The %BC, $W_{BC}$, $W_{IB}$ and $W_{NC}$ in Equation (1) are the percent yield of biochar, the weight of biochar, the weight of input biomass and the weight of non-carbonized biomass, respectively (Kongnine *et al.*, 2020). The ideal charcoal yield during the pyrolysis process would be 35% of the weight of the original raw material (Meyer, 2009). The pyrolysis gas produced by the 50L-HBGS inferred by the loss of total weight after the pyrolysis process, which was estimated by Equation (2), i.e.,

$$\%PG = \frac{W_{IB} - W_{SY}}{W_{IB}} \times 100 \quad (2)$$

where *%PG* and $W_{SY}$ are the percent of produced gas and the weight of total solids yields, respectively (Intagun *et al.*, 2018).

### *2.3 Bamboo Feedstock Preparation*

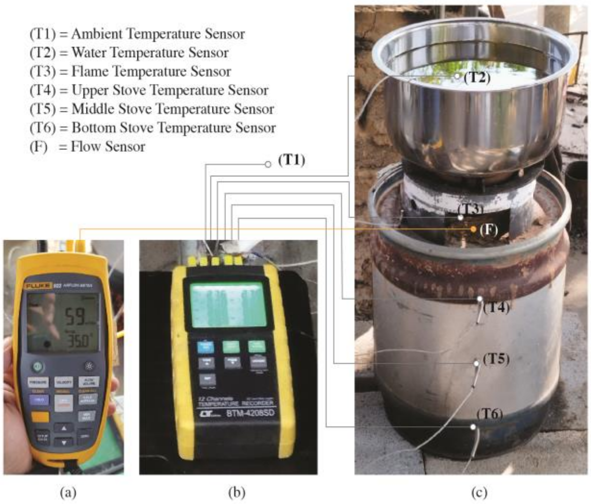


**Fig. 2** Monitoring of the 50L-HBGS: (a) the air flow meter (b) Temperature data recorder (c) position of sensors during experiment

Biochar production can use a variety of organic materials or waste feedstocks, such as citrus peel fruit (Selvarajoo *et al*., 2022), sewage sludge, and pine needles (Fatima *et al*. 2022), even microalgae, etc. (Chen *et al*., 2022). However, bamboo is one of the fastest growing plants in the world (Jeffery *et al*., 2023) and has covered a large area in many countries around the world (Sawarkar *et al*., 2023; Adeniyi *et al*., 2023), especially in Asia such as China, India, even Thailand, etc. (Sawarkar *et al*., 2020). The main components of bamboo wood are hemicelluloses, cellulose, and lignin (Rusch *et al*., 2023), which those are significant for biochar production by pyrolysis stove (Tomczyk *et al*., 2020). According to Chen *et al*. (2010), bamboo biochar has a surface area and micropore size that are approximately 4 and 10 times larger than those in regular biochar. Moreover, with the fact that biochar from bamboo is more stable than from grasses, sludge, and husks (Cely *et al*., 2014; Hilscher *et al*., 2009; Zimmerman, 2010) and has quality in the range that can create value-added healthcare products, such as applications for skin treatments, medical products (Sawarkar *et al*., 2023; Kumar *et al*., 2023), or even the electrical electrode, etc. (Sayed *et al*., 2022), bamboo was used as the feedstock for this research. In the study, bamboo wood chunks with a moisture content of 9.4% on a dry basis, a length of 10 cm, and a diameter of 3.5 cm were prepared for experiments in the 50L-HBGS.

### *2.4 Statistical Analysis Method*

The stove temperature data of the NCCS case and the ECCS case that had been tested in the 50L-HBGS were analyzed by the statistical technique, so-called one-way analysis of variance (ANOVA). The ANOVA had been applied in biochar research, such as by Ippolito *et al*. (2020), Muzyka *et al*. (2023), and Bonanomi *et al*. (2023) to define the differences in groups of variables. The comparison of the airflow rate, and heat rate between the NCCS and ECCS was done using the paired sample t-test due to a single paired comparison (Baldoni *et al*., 2023; Prakongkep *et al*., 2020; Bonanomi *et al*., 2023). The analysis in this study was performed by SPSS program, at a significant level of $P < 0.05$ to compare differences and justify the effects of the combustion core type on an improvement of stove characteristics.

## 3. Experimental Procedure

### *3.1 Biochar Stove Testing*

The three experiments of biochar production were performed in order to collecting information of airflows, temperatures and biochar products which gained by uses the NCCS and ECCS in the 50L-HBGS. After the NCCS and ECCS were integrated into the 50L-HBGS, 9 kg of bamboo wood chunks ($W_{IB}$) were added to the pyrolysis section, and 3 kg added in to the combustion core of each case, which called as the NCCS case and the ECCS case for this study, respectively. Afterward, six K-type temperature sensors were then integrated into each point (Figure 2c). All temperature sensors were connected to the PCE multichannel data logger (Figure 2b), which automatically records every 5 minutes. Since the heats for pyrolysis is generated by fuel wood in the combustion core; then, the 3 kg of bamboo firewood was prepared inside the cores. The NCCS has a larger core volume; it contained all 3 kg in a fill. Conversely, the ECCS has a smaller core volume, and it took more than one filling in the core while the stove was processing, which makes it uncomfortable to use. After everything was prepared, the stoves started to ignite, and data monitoring was started. The experiment was conducted until no more pyrolysis gas is emitted from the stove. In the meantime, the total amount of firewood used in the core were recorded. When the kiln had cooled down, the biochar and the total solid weight in the stove were measured.

In the test of the differences in air flow, due to the very high gas flow rate in the core of both cases during pyrolysis gas formation, the airflow was recorded in the initial interval of 45 minutes after the stoves were lit only. The differences in the air flow rate of the combustion cores was classified by using the measured data, which obtained with the Fluke 922 air flow meter (Figure 2a).

### *3.2 Biochar Characterization*

After the experiments, the quality of bamboo biochar was characterized by using Fourier transform infrared spectroscopy (FTIR), model Frontier and Spotlight 200i from Perkin Elmer, USA, which runs in the range 600–7,800 $cm^{-1}$. In the beginning, the biochar samples were examined for electrical resistivity, then the biochar sample in each group with the lowest resistivity was chosen to be placed on the ATR diamond crystal plate, coated with powder, and then characterized using the Frontier and Spotlight 200i. The relation between wavelength and percent transmittance obtained from the biochar sample can reflect the different of chemical components of the biochar.

After the test, the differences in surface functional groups were defined. This method also was examined to see how the pyrolysis temperature affected the components remaining in Biochar. Then, the pore size and element content of the biochar were determined by using the scanning electron microscopy (SEM), model TM4000Plus, by Hitachi, and energy dispersive X-ray spectroscopy (EDS). SEM and EDS were used to examine the surface morphology and chemical composition of the bamboo biomass sample from the NCCS case, which is important to define whether it is in the range for application as an adsorption material or not. Finally, proximate analysis was also performed for further explanation of the distinction between the biochar from the NCCS case and the ECCS case. The study was performed according to the standards set by ASTM D1037 (1991), ASTM D3172, ASTM D2017 (1998), and ASTM E1755, respectively. The parameters studied in the proximate analysis were the moisture content, volatile matter content (VOC), ash content, and fixed carbon content.

## 4. Results and Discussions

### 4.1 Combustion Core Air Flow

In the experiment, stoves were ignited at the top of the combustion cores, and then fuel wood was burned down to the bottom section. The heat was transferred to the bamboo wood in the pyrolysis section (outer cylinder), creating pyrolysis gas and biochar. The results of the average air flow rate from three tests, obtained by using the Fluke 922 air flow meter and measured after the stoves were lit, are shown in Figure 3. The average airflow, from 48 data points, before the continuous pyrolysis was started was 57.25 $m^3/h$ for the NCCS case (Table 1), which on average is 62.24% higher than the ECCS case. The result after the paired sample t-test of the airflows was performed (Table 2) indicates that the airflow rate in the combustion core of the NCCS case is significantly different from the ECCS case (P value = 0.000). The higher airflow in the NCCS relates to the physical shape of the core, which has a large lower air inlet volume (Figures 1b and 1c), which is important for better low-temperature air inlet flow into the core during high-temperature combustion. It is clarified that the application of the NCCS to the 50L-HBGS has significantly improved the passive airflow rate in the combustion core of the stove.

### 4.2 Pyrolysis Temperature Profiles

The average temperature data after stoves were three-time experiments are shown in Figures 4 and 5. The profiles $T_l$ (green), $T_m$ (red), and $T_u$ (blue) represent to temperature at the lower, middle, and upper pyrolysis sections of the stove, respectively. And $T_f$ (orange) is the flame temperature of the stove. The information from Figure 4 shows that temperature profiles in the ECCS case has more high fluctuation, especially, it clearly exposed in $F_t$. The high fluctuations, during the 75 minutes after the stove was lit, were caused by the physical design of the core, which has a small air inlet section (Figure 1a), causing it to deliver a low airflow rate, which is around 25 $m^3/h$ (Figure 3), combined with the ash blockage in the core, which results in a mismatch of air in combustion and misfires in the combustion core. Moreover, with a small volume of the core for contain the fuel wood, the stove had to be operated by the user to increase the air flow and enhance the flame, which made it uncomfortable to use and prolonged the time to produce biochar. The syngas burns continuously in the core at 75 minutes after ignition, and then it takes 65 minutes to finish the gas discharge (Figure 4). On average, the stove took an overall 140 minutes to finish ejecting syngas. From Table 3, the maximum average of flame temperature ($T_{f, ECCS}$) in this case is 890.23 °C. At the pyrolysis zone temperatures, the $T_{u, ECCS}$ and $T_{m, ECCS}$ have a maximum average value over 500 °C for approximately 30 minutes, which implies that bamboo chunks at the middle and upper zones of the stove have converted to biochar (Lee *et al*., 2013). However, the lower part temperature ($T_{l, ECCS}$) of the stove has a maximum average temperature of 365.73 °C, which is not enough to remove the tar and convert all bamboo chunks in this zone to biochar.

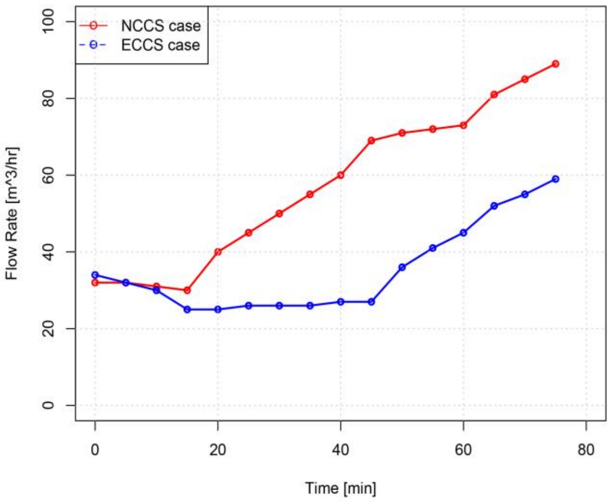


**Fig. 3** The average air flow rate at outlet section of the combustion core from three experiments

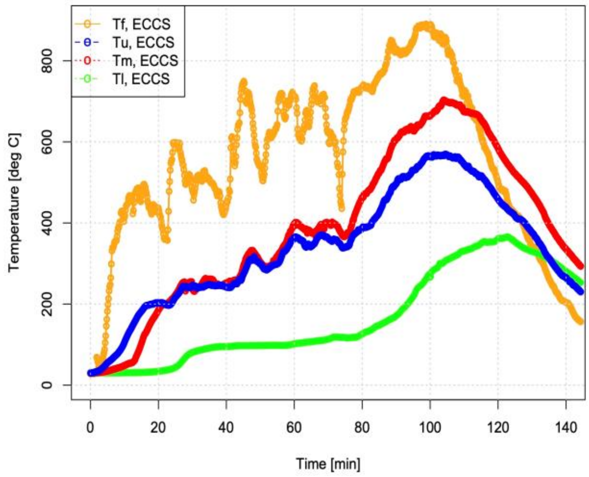


**Fig. 4** Average temperature profiles of the ECCS case from three experiments

**Table 1**
Sample statistics of the airflow

| | M | N | SD | Std. Error Mean |
|---|---|---|---|---|
| NCCS | 57.25 | 48 | 20.21 | 2.91 |
| ECCS | 35.31 | 48 | 11.64 | 1.68 |

**Table 2**
Paired sample t-test of the airflow of the NCCS and ECCS

| Paired Differences | | | | | t | df | Sig. (2-tailed) |
|---|---|---|---|---|---|---|---|
| M | SD | Std. Error M | 95% Confidence Interval of the Difference | | | | |
| | | | Lower | upper | | | |
| 21.93 | 14.20 | 2.05 | 17.81 | 26.06 | 10.69 | 47 | 0.000 |

In the NCCS case (Figure 5), due to an improvement in airflow rates in the combustion core and a sufficient containment volume of fuel wood in the core (one-time filled), the growth of the pyrolysis temperature profiles in the stove is more stable than in the ECCS case. Even if the flame temperature decreased 35 minutes after lighting due to the ash blockage, the large air inlet volume of the core (Figure 1b) and sufficient fuel wood contained inside could create high airflow pressure, resulting in continued flaming throughout the process without the need for user intervention. Implies that the production method of the 50L-HBGS has been changed. The pyrolysis starts 45 minutes after lighting and ends 75 minutes later. The total duration from start ignition to end of pyrolysis gas discharge is on average 120 minutes, which implies that it took a shorter biochar production time than the ECCS case. The descriptive data of temperature from three experiments in the NCCS case is shown in Table 3. The maximum average flame temperature ($T_{f, NCCS}$) in this case is 909.93 °C. The maximum average of pyrolysis temperatures $T_{l, NCCS}$, $T_{m, NCCS}$, and $T_{u, NCCS}$ are 560.5, 655.1, and 788.7 °C, respectively, which are all higher than in the ECCS case. The pyrolysis temperature in this case

**Table 3**
Descriptive data of average temperature in each position between the NCCS case and EECCS case

| Temp. | N | M | SD | SE | 95% Confidence Interval for Mean | | Min | Max |
|---|---|---|---|---|---|---|---|---|
| | | | | | Lower Bound | Upper Bound | | |
| $T_{l, NCCS}$ | 867 | 244.65 | 177.61 | 6.03 | 232.81 | 256.49 | 32.77 | 602.00 |
| $T_{l, ECCS}$ | 867 | 167.64 | 113.98 | 3.87 | 160.04 | 175.24 | 30.13 | 365.73 |
| Total | 1734 | 206.14 | 154.07 | 3.70 | 198.89 | 213.40 | 30.13 | 602.00 |
| $T_{m,NCCS}$ | 867 | 358.96 | 209.08 | 7.10 | 345.02 | 372.89 | 36.83 | 778.17 |
| $T_{m, ECCS}$ | 867 | 386.25 | 192.35 | 6.53 | 373.43 | 399.08 | 29.77 | 703.23 |
| Total | 1734 | 372.60 | 201.29 | 4.83 | 363.12 | 382.09 | 29.77 | 778.17 |
| $T_{u, NCCS}$ | 867 | 309.54 | 146.21 | 4.96 | 299.80 | 319.29 | 32.63 | 606.80 |
| $T_{u, ECCS}$ | 867 | 337.48 | 139.16 | 4.72 | 328.20 | 346.76 | 30.10 | 569.70 |
| Total | 1734 | 323.51 | 143.37 | 3.44 | 316.76 | 330.27 | 30.10 | 606.80 |
| $T_{f, NCCS}$ | 867 | 481.26 | 234.56 | 7.96 | 465.62 | 496.89 | 76.73 | 909.93 |
| $T_{f, ECCS}$ | 867 | 557.19 | 206.05 | 6.99 | 543.45 | 570.92 | 27.90 | 890.23 |
| Total | 1734 | 519.22 | 223.95 | 5.37 | 508.67 | 529.77 | 27.90 | 909.93 |
| All | 63936 | 355.37 | 215.26 | 2.58 | 350.30 | 360.44 | 27.90 | 909.93 |

**Table 4**
Anova analysis of the average temperature between the NCCS case and EECCS case

| | | Sum of Squares | df | Mean Square | F | Sig. |
|---|---|---|---|---|---|---|
| $T_l$ | Between Groups | 2.570E6 | 1 | 2.570E6 | 115.443 | 0.000 |
| | Within Groups | 3.857E7 | 1732 | 22269.73 | | |
| | Total | 4.114E7 | 1733 | | | |
| $T_m$ | Between Groups | 3.230E5 | 1 | 3.230E5 | 8.005 | 0.005 |
| | Within Groups | 6.990E7 | 1732 | 40357.81 | | |
| | Total | 7.022E7 | 1733 | | | |
| $T_u$ | Between Groups | 3.382E5 | 1 | 3.382E5 | 16.604 | 0.000 |
| | Within Groups | 3.529E7 | 1732 | 20374.074 | | |
| | Total | 3.563E7 | 1733 | | | |
| $T_f$ | Between Groups | 2.499E6 | 1 | 12.499E6 | 51.275 | 0.000 |
| | Within Groups | 8.442E7 | 1732 | 48740.197 | | |
| | Total | 8.692E7 | 1733 | | | |
| All | Between Groups | 9.317E7 | 7 | 1.331E7 | 404.141 | 0.000 |
| | Within Groups | 2.282E8 | 6928 | 32935.456 | | |
| | Total | 3.214E8 | 6935 | | | |

reaches over 500 °C, which is in the range of optimum biochar production (Brady *et al*., 2008; Klüpfel *et al*., 2014; Lehmann, 2015) and sufficient to remove volatile matter and develop pore structure (Lee *et al*., 2013).

Comparative of the NCCS and ECCS by used the ANOVA statistics gives descriptive data of an average temperature in each point as shown in Table 3. In which the maximum average of $T_{l, NCCS}$ is 602.00 °C, which is 64.6% higher than the maximum average of $T_{l, ECCS}$ (Figure 6). The $T_{l, NCCS}$ reached over 500 °C for 20 minutes during peak of pyrolysis is (Figure 5), which is important to produce high amount of fixed carbon, as well as reduces of volatile matter contain in biochar (Lee *et al*., 2013). Test of the ANOVA result (Table 4) indicated that all paired of $T_l$, $T_m$, $T_u$ and $T_f$ have significantly difference ($P < 0.05$). The largest different of mean value found in the lower zone temperature ($T_l$), with highest F value of 115.443. The 2nd, and 3rd difference found in $T_f$ and $T_u$, respectively. Whereas $T_m$ is smallest in difference. Moreover, the bar chart in Figure 6 shows

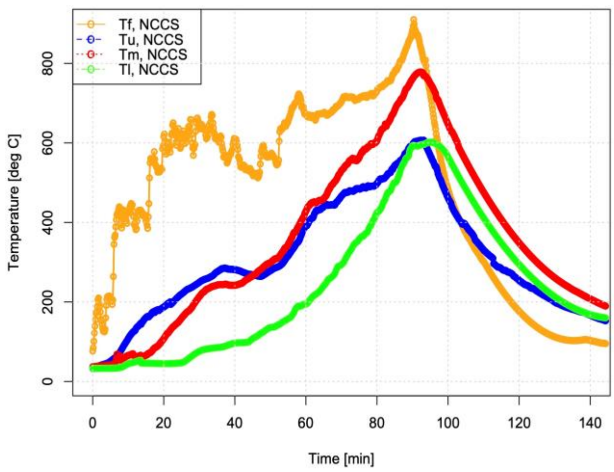


**Fig. 5** Average temperature profiles of the NCCS case from three experiments

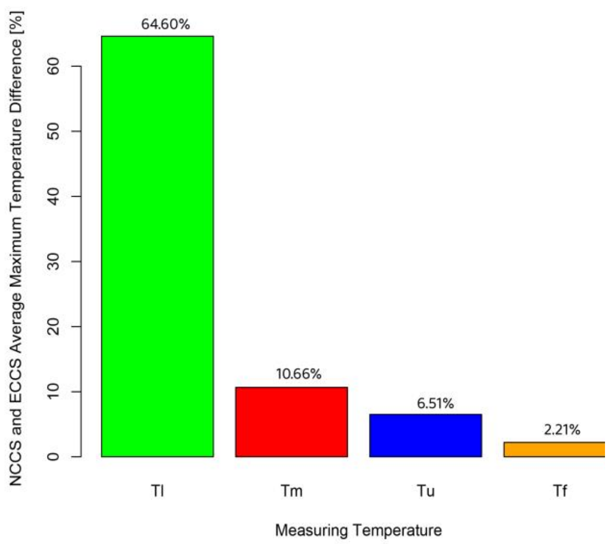


**Fig. 6** The percent difference of maximum average temperature between the NCCS case and the ECCS case

**Table 5**
Descriptive data of stove's average heat rate in each position

| Position | N | M | SD | SE (*E-3) | 95% Confidence Interval for Mean Lower Bound | Upper Bound | Min | Max |
|---|---|---|---|---|---|---|---|---|
| @$T_{l, NCCS}$ | 867 | 0.0703 | 0.0635 | 2.15 | 0.0661 | 0.0745 | 0.000 | 0.5098 |
| @$T_{l, ECCS}$ | 867 | 0.0329 | 0.0422 | 1.43 | 0.0301 | 0.0357 | 0.000 | 0.6382 |
| Total | 1734 | 0.0516 | 0.0570 | 1.37 | 0.0489 | 0.0543 | 0.000 | 0.6382 |
| @$T_{m, NCCS}$ | 867 | 0.1004 | 0.0781 | 2.65 | 0.0952 | 0.1056 | 0.000 | 0.7895 |
| @$T_{m, ECCS}$ | 867 | 0.1102 | 0.0998 | 3.38 | 0.1036 | 0.1169 | 0.000 | 0.8666 |
| Total | 1734 | 0.1053 | 0.0897 | 2.15 | 0.1011 | 0.1095 | 0.000 | 0.8666 |
| @$T_{u, NCCS}$ | 867 | 0.0796 | 0.0647 | 2.19 | 0.0753 | 0.0839 | 0.000 | 0.4509 |
| @$T_{u, ECCS}$ | 867 | 0.0851 | 0.0644 | 2.18 | 0.0815 | 0.0901 | 0.000 | 0.3745 |
| Total | 1734 | 0.0827 | 0.0646 | 1.55 | 0.0797 | 0.0857 | 0.000 | 0.4509 |
| @All | 5202 | 0.7991 | 0.7513 | 1.04 | 0.7787 | 0.0819 | 0.000 | 0.8666 |

**Table 6**
Anova analysis of the stove's average heat rate in each position

| | | Sum of Squares | df | Mean Square | F | Sig. |
|---|---|---|---|---|---|---|
| @$T_l$ | Between Groups | 0.606 | 1 | 0.606 | 208.220 | 0.000 |
| | Within Groups | 5.041 | 1732 | 0.003 | | |
| | Total | 5.647 | 1733 | | | |
| @$T_m$ | Between Groups | 0.042 | 1 | 0.042 | 5.248 | 0.022 |
| | Within Groups | 13.915 | 1732 | 0.008 | | |
| | Total | 13.975 | 1733 | | | |
| @$T_u$ | Between Groups | 0.016 | 1 | 0.016 | 3.907 | 0.048 |
| | Within Groups | 7.217 | 1732 | 0.004 | | |
| | Total | 7.234 | 1733 | | | |
| @All | Between Groups | 3.185 | 5 | 0.637 | 126.471 | 0.000 |
| | Within Groups | 26.173 | 5196 | 0.005 | | |
| | Total | 29.358 | 5201 | | | |

clearly that the major improvement is in the lower zone temperature ($T_l$) of the pyrolysis chamber. These results indicate that the pyrolysis temperatures and the profile characteristics of the 50L-HBGS have been improved by using the NCCS.

### *4.3. Heat Rate Analysis*

Figures 7 and 8 show the heat rates at any position along the 50L-HBGS in both cases. The upper, middle, and lower sections of the 50L-HBGS are indicated by the red, blue, and green lines, respectively. The data in Figures 7 and 8 reveals that there are two key distinctions between the ECCS and NCCS cases: the first is the value of the heat rates, and the second is the profile pattern. The descriptive data in Table 5 indicates that the heats rate in both cases is less than 10 °C/min, implies that the test was carried out in the range of the slow-pyrolysis process, which is favorable for produces biochar (Wang *et al.,* 2018; Zhao *et al.,* 2019; Shen & Wu, 2023; Abdullha *et al.*, 2023). In both cases, there has discernible variation in the heat rate at the upper area of the stove (@$T_U$), which is confirmed by the ANOVA test data in Table 6 (P = 0.048). Moreover, there is a substantial difference between the heat rates at the middle (P = 0.002) and lower sections (P = 0.000). The heat rate at lower section of the NCCS case is higher than the ECCS case, however, the heat rate is lesser in the middle and upper section.

The heat rate characteristics above are because the size of the core puncher in the ECCS case is bigger than in the NCCS case, which results in a higher volume of pyrolysis gas dissipating to burn in the combustion core, and results to a higher heat rate transfer through the wall of the middle section (red) and upper section (blue) of the stove, as shown in Figure 7. However, with the high gas discharge, which causes insufficient time for organic vapor to react with the

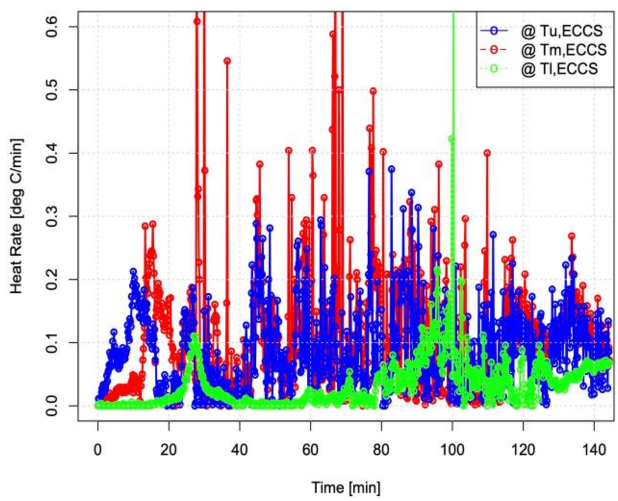

**Fig. 7** The average heat rate of the 50L-HBGS with the ECCS

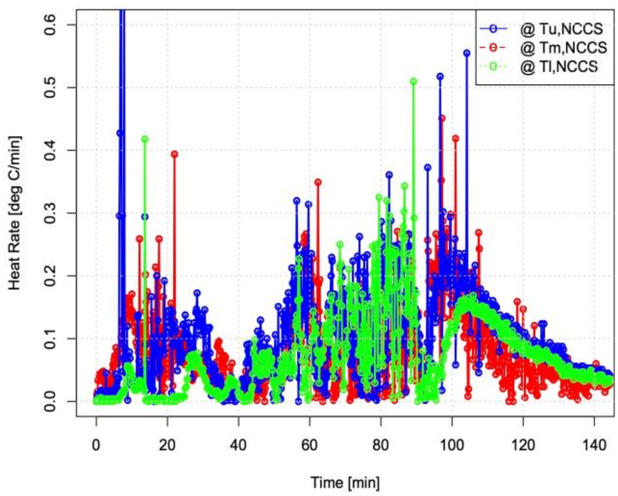

**Fig. 8** The average heat rate of the 50L-HBGS with the NCCS

carbonaceous material (Antal & Grønli, 2003; Crombie & Mašek, 2015) at the lower part of the stove, and the straight combustion core design, gives the ECCS lacks of surface area and time to transport heat in the flame to the lower portion of the pyrolysis chamber, then the heat rate at the lower pyrolysis zone is not sufficient (green line in Figure 7) for the decomposition of the wood chunk, resulting in the remaining of tar and unburned bamboo at the end (Figure 9a).

In the NCCS case, the new design of the combustion core has a larger volume and surface area at the lower section (Figure 1b). The sensible heat from fuel wood combustion at the wall of the lower core causes an increased heat rate through the large wall of the lower core to the lower pyrolysis zone, as shown by the green lines in Figure 8. Moreover, large air inlet section of the core provides sufficient airflow for burning gas and wood fuel in the combustion core, therefore the heat rate profile pattern is less fluctuation than in the ECCS case. However, it has smaller size of the core puncher at lower core, effects to the lower rate of pyrolysis gas discharge to the combustion core. The lower pyrolysis gas discharge during start of pyrolysis (at 50-75 minutes in Figure 5) allows organic vapor to have more time to react with the carbonaceous material, forming more $H_2$ and CO with exothermic heat, result to the higher in maximum temperature and pressure at the final pyrolysis process (Antal & Grønli, 2003; Crombie & Mašek, 2015).

### 4.4 Biochar Yield and Pyrolysis Gas Yield

From the stove testing, it was found that the weight of total solid yield ($W_{SY}$) and the weight of biochar yield ($W_{BC}$) in the NCCS case are 2.50 and 2.45 kg, respectively, which is slightly lower than the ECCS case (Table 7). The ECCS case seems to be more dominant than the NCCS case in this point; however, the physical details of biochar from the ECCS case in Figure 9a shows the contaminate of tar and part of unburned bamboo wood chunk (0.35 kg). Figure 9b simply indicates that the biochar products from the NCCS case are better than those from the ECCS case, where all bamboo wood chunks and tar are converted to biochar and pyrolysis gas. With the %BG yields by the NCCS is 27.37%, shown in Table 7, indicates that production of biochar by the NCCS case is in the rage of %BG gained by the 50L-HBGS, as reference to Maneekhat and Khamdaeng (2022), Sittioad *et al.* (2022) and Panyoyai *et al.* (2019). However, it was slightly lower due to the improvement in pyrolysis temperature in the stove and the difference in feedstock used in the experiment.

Nonetheless, the results of higher %PG and lower %BG in the NCCS case than the ECCS case can be explained by the fact that the modified combustion chamber in the NCCS case effects an increasing pyrolysis temperature (esp. at the lower section), which is sufficient to decompose all of the bamboo wood chunks in the pyrolysis chamber and convert tar to pyrolysis gas and char (Ojolo *et al.*, 2013). This concludes that apply the NCCS in the stove results to increase the %PG but decrease the %BC, compared to the ECCS.

**Fig. 9** Biochar gained form the 50L-HBGS; (a) with ECCS (b) with NCCS

**Table 7**
Weights parameter of biochar (three average data)

| Parameter | ECCS case | NCCS case |
|---|---|---|
| $W_{BC}$ (kg) | 2.60 | 2.45 |
| $W_{SY}$ (kg) | 2.96 | 2.50 |
| $W_{NC}$ (kg) | 0.36 | 0.05 |
| $W_{IB}$ (kg) | 9.00 | 9.00 |
| %BC | 30.00 | 27.37 |
| %PG | 67.11 | 72.22 |

### 4.5 Biochar Surface Function Group

FTIR analysis revealed that the pyrolysis temperature had a remarkable impact on the functional groups of biochar. FTIR spectra of the bamboo biochar from the 50L-HBGS are shown in Figure 10. The BB-C1 is a spectra line of biochar from the ECCS case. And BB-C2 is the spectra line of biochar from the NCCS case. Several peaks of Both BB-C1 and BB-C2 biochar disappeared during the pyrolysis process (from 200 °C) due to hemicellulose beginning to demonstrate pyrolysis, as denoted by the characteristic's bands at 3335-3483 $cm^{-1}$ (O–H stretching vibrations of lignin, hemicellulose, and cellulose), 1711 $cm^{-1}$ (C=O stretching of lignin), and 1610 $cm^{-1}$ (C=C asymmetric stretching of lignin) which were caused by $H_2O$ and $CO_2$. The absorption peak at 1378 $cm^{-1}$ (C-O stretching of hemicellulose) suggests the ether contains in the biochar. Absorption bands at 785 $cm^{-1}$ may have been caused by the bending vibrations of the C-H atom in polycyclic or substituted aromatic groups (Zhao *et al.*, 2019). All absorption peaks displayed a rising pattern at 350 °C, alongside the breakdown of hemicellulose, cellulose, and lignin. The absorption bands at 2362 $cm^{-1}$ (C-C asymmetric stretching of hemicellulose), 2850 $cm^{-1}$ ($CH_2$ stretching vibrations for aliphatic $CH_3$ and $CH_2$ groups), and 2923 $cm^{-1}$ (CO and $CH_4$) were brought on by CO and $CH_4$, primarily from broken C-O bonds and C=O.

The transmittance at 1317 $cm^{-1}$ is due to the occurrence of aromatics with C-C stretching (ester and phenol) (Abdullah *et al.*, 2020; Grover *et al.*, 2002; Armynah *et al.*, 2018).

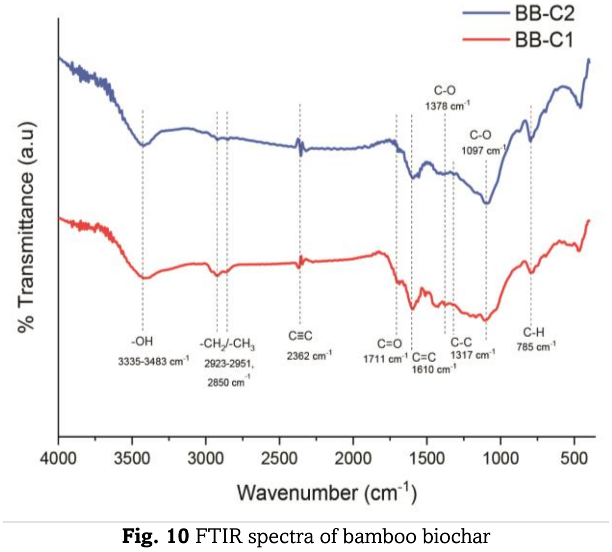

**Fig. 10** FTIR spectra of bamboo biochar

And transmittance at 1097 cm$^{-1}$ is due to symmetric C-O stretching and C-OH bending of hemicellulose, cellulose, and lignin (Armynah *et al.*, 2019). The change in temperature in biochar products affect the decomposition of cellulose, hemicellulose, and lignin. The volatile matter emission from biochar increases with pyrolysis temperature (Enders *et al.*, 2012; Crombie *et al.*, 2013). The compounds containing C-C and C-H stretching or bending functional groups were prevalent in each bamboo subfamily. When the temperature reached 600 °C, the $CO_2$ absorption peaks were almost at their maximum absorbance (i.e., at the lignin decomposition stage), whereas the other component's absorption strength decreased, this suggested that the reaction was complete (Zhao *et al.*, 2019). In the case of the BB-C2, the spectral bands at 2923–2951, 2850, 2362, 1711, 1610, and 1378 cm$^{-1}$ clearly decreased as the maximum temperature of the pyrolysis zone increased. This result indicates that the NCCS effects an increase in the 50L-HBGS temperature, which improves the carbon content of biochar (Sahoo *et al.*, 2021).

*4.6 The surface morphologies and chemical composition*

The BB-C2 sample has a less rough or cracked outside surface, as seen in Figures 11(a) and 11(a-1), due to less fluctuation of temperature while slow low heating rates occurred (Ong *et al.*, 2021; Zhang *et al.*, 2020) during the pyrolysis process of the stove, and heat is likely to transfer through the longitudinal direction rather than in the radius direction of bamboo wood chunks (Kalderis *et al.*, 2023; Pinisakul *et al.*, 2023). However, increasing pyrolysis temperature results in improved total surface and pore volumes of biochar (Binh *et al.*, 2022; Hettithanthri *et al.*, 2023; Faraji *et al.*, 2023), but a thinner wall of the pore was found due to the decomposition of hemicellulose, cellulose, and lignin with increased temperature (Figures 11b and 11b-1). The distribution of porosity is larger than 50 nm, which implies that pore size is in the macropore (Chen *et al.*, 2023), which relates to an increase in the calcination temperature of the NCCS case. Moreover, according to Yang *et al.* (2016), Viglaová *et al.* (2018), and Ji *et al.* (2022), the pore of biochar in the NCCS case is in the range of micropore and macropore size, indicating that it is suitable for adsorption applications (Xu *et al.*, 2017). While the BB-C1 and BB-C2 samples' elemental compositions, as determined by EDS analysis, indicate that carbon, oxygen, silicon, and potassium are the main components, as seen in Figure 12. The nitrogen concentration vanishes from the graphs in both situations due to the prolonged pyrolysis process (Armynah *et al.*, 2019). The biochar created by the 50L-HBGS with the NCCS is more suited for soil treatment than the biochar produced by the ECCS case, according to the dominating potassium observed in the biochar from the NCCS case (Oram *et al.*, 2014; Wang *et al.*, 2018).

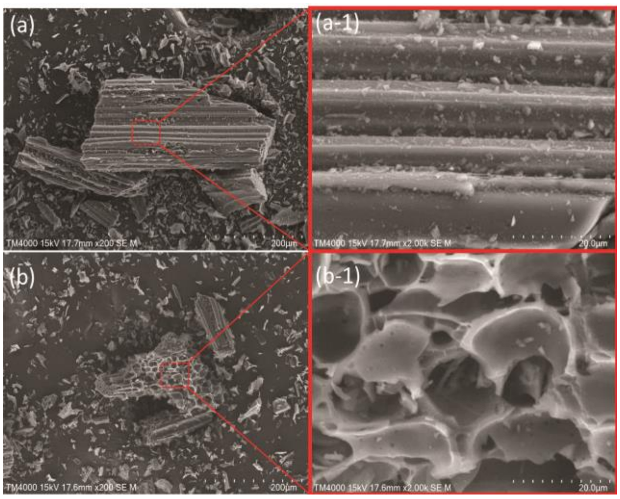


**Fig. 11** SEM images of BB-C2 surface (a, a-1) and cross-section (b, b-1) with different magnification

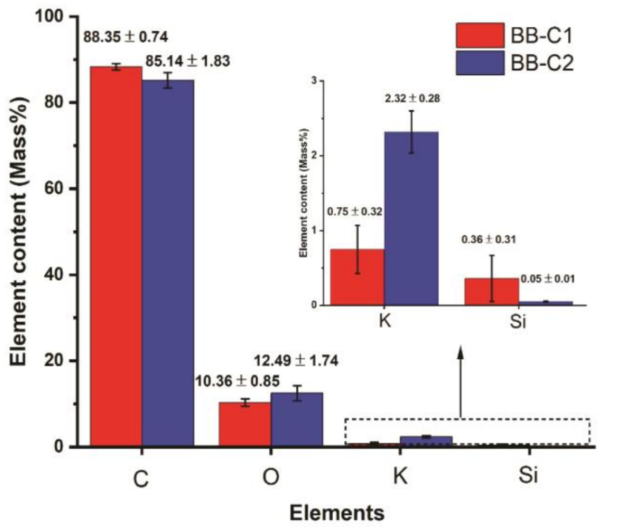


**Fig. 12** The elements in BB-C1 and BB-C2 by the EDS technique

*4.7 Proximate Analysis*

Table 8 shows the proximate analysis results. The results from the test show that the dry bamboo wood chunk is appropriate for the experiment; it has a 9.4 ± 0.11% moisture content. The VOC contained in the bamboo wood chunk is 76.0 ± 0.76%. Ash and Fixed Carbon found in the test are 1.5 ± 0.13% and 13.1 ± 0.7%, respectively. The biochar obtained from the NCCS case (sample BB-C2) has a fixed carbon content of 74.2 ± 3.6%, which is approximately 50% higher than the biochar obtained from the ECCS case (sample BB-C1). The improvement of fixed carbon content indicates that the NCCS is beneficial for improving the carbon sequential characteristic of the biochar obtained from the stove (Ogawa *et al.*, 2006; Yablonovitch and Deckman, 2023). Moreover, 9.5 ± 0.75% of the VOC in the BB-C2, which is lower than in the BB-C1, indicated that the purity of biochar can be improved by using the NCCS instead of the ECCS in the 50L-HBGS.

*4.8 Limitation of the study*

Even though the study found that the 50L-HBGS with the NCCS served continuous burning and deployed of remining tar and unburned bamboo wood at the end, however, there still have

**Table 8**
The proximate analysis data of bamboo biochar

| Sample | Moisture Content (%) | VOC (%) | Ash (%) | Fixed Carbon (%) |
|---|---|---|---|---|
| BB-C1 | 4.1 ± 0.21 | 36.4 ± 5.75 | 10.1 ± 3.87 | 49.5 ± 9.3 |
| BB-C2 | 4.0 ± 0.45 | 9.5 ± 0.75 | 12.3 ± 3.53 | 74.2 ± 3.6 |
| BB wood | 9.4 ± 0.11 | 76.0 ± 0.76 | 1.5 ± 0.13 | 13.1 ± 0.7 |

limitation of the study due to the type, size and humidity of fuel wood was used in the specific range. Further study should be concerning to the varying in the other range of bamboo wood size and humidity, as well as different type of fuel wood uses in the study. Since the water boiling Test method is not suitable for application in the study, an option of the thermal performance investigation is a key that needs to be focused on.

## 5. Conclusion

The study of the development of the combustion core of the 50L-HBGS was to address the problems of the existing 50L-HBGS in Thailand, which are discontinuous combustion during the ignition process, wood pieces remaining at the end of combustion, and the problem of liquid tar contamination of biochar products. The combustion characteristic result indicated that the NCCS case provided continues to burn better than the ECCS case during the ignition process because the airflow rate in the combustion core was improved. In addition, the stove's temperature was higher than 500 °C during the pyrolysis process, which resulted in the removal of the liquid tar and left no unburned wood pieces at the end. The characterization result showed that the NCCS case produced biochar in the range of micropore and macropore sizes with a higher purity and fixed carbon content than the ECCS case. And, because of the way the volatile organic compounds (VOCs) in the biochar derived from the NCCS case were lower than that of the ECCS case, the biochar obtained from the NCCS case had better characteristics for adsorption, soil treatment, and other agricultural uses. The percentage improvement of fixed carbon contained in the biochar from the NCCS case is also advantageous for future carbon sequestration applications. This study shows that applying the NCCS to the 5L-HBGS results improves both the stove's combustion characteristics and the quality of bamboo biochar production. This could be beneficial for the promotion of the stove under the concept of the United Nations Sustainable Development Group (UNSDG), such as growing more food in poor soils by using biochar to reduce hunger, replacing chemicals in agriculture with biochar for good health and well-being, low-cost filtration medium by biochar for clean water and sanitation, etc.

## Acknowledgments

We are grateful to Associated Prof. Dr. Paveena Laokul's staff and the Central Laboratory at Mahasarakham University for providing valuable support on FTIR and SEM analysis in this project, and we are especially grateful to Mahasarakham University for financial and facility support.

**Author Contributions**: S.C.: Conceptualization, methodology, data monitoring, formal analysis, writing—original draft, R.C.; supervision, resources, J.S.; statistical analysis supervision, J.P.; review and editing, validation, A.S.; Conceptualization, supervision, writing—review and editing, project administration, validation. All authors have read and agreed to the published version of the manuscript.

**Funding:** This research was financially supported by Mahasarakham University.

**Conflicts of Interest:** The authors declare no conflict of interest.

## References

Abdullah, A., Ahmed, A., Akhter, P., Razzaq, A., Zafar, M., Hussain, M., ... & Park, Y. K. (2020). Bioenergy potential and thermochemical characterization of lignocellulosic biomass residues available in Pakistan. *Korean Journal of Chemical Engineering*, 37, 1899-1906, https://doi.org/10.1007/s11814-020-0624-0

Abdullah, N., Taib, R. M., Aziz, N. S. M., Omar, M. R., & Disa, N. M. (2023). Banana pseudo-stem biochar derived from slow and fast pyrolysis process. *Heliyon*, 9(1). https://doi.org/10.1016/j.heliyon.2023.e12940

Adeniyi, A. G., Adeyanju, C. A., Iwuozor, K. O., Odeyemi, S. O., Emenike, E. C., Ogunniyi, S., & Te-Erebe, D. K. (2023). Retort carbonization of bamboo (Bambusa vulgaris) waste for thermal energy recovery. *Clean Technologies and Environmental Policy*, 25(3), 937-947. https://doi.org/10.1007/s10098-022-02415-w

Ajieh, M. U., Owamah, H. I., Edomwonyi-Otu, L. C., Ajieh, G. I., Aduba, P., Owebor, K., & Ikpeseni, S. C. (2023). Characteristics of fuelwood perturbation and effects on carbon monoxide and particulate pollutants emission from cookstoves in Nigeria. *Energy for Sustainable Development*, 72, 151-161. https://doi.org/10.1016/j.esd.2022.12.008

Antal, M. J., & Grønli, M. (2003). The art, science, and technology of charcoal production. *Industrial & engineering chemistry research*, 42(8), 1619-1640, https://doi.org/10.1021/ie0207919

Armynah, B., Atika, Djafar, Z., Piarah, W. H., & Tahir, D. (2018, March). Analysis of chemical and physical properties of biochar from rice husk biomass. *In Journal of Physics: Conference Series* (Vol. 979, p. 012038), IOP Publishing, https://doi.org/10.1088/1742-6596/979/1/012038

Armynah, B., Tahir, D., Tandilayuk, M., Djafar, Z., & Piarah, W. H. (2019). Potentials of biochars derived from bamboo leaf biomass as energy sources: effect of temperature and time of heating. International *Journal of Biomaterials*, 2019, https://doi.org/10.1155/2019/3526145

Baldoni, N., Francioni, M., Trozzo, L., Toderi, M., Fornasier, F., D'Ottavio, P., ... & Cocco, S. (2023). Effect of wood gasification biochar on soil physicochemical properties and enzyme activities, and on crop yield in a wheat-production system with sub-alkaline soil. *Biomass and Bioenergy*, 176, 106914. https://doi.org/10.1016/j.biombioe.2023.106914

Balmuk, G., Videgain, M., Manyà, J. J., Duman, G., & Yanik, J. (2023). Effects of pyrolysis temperature and pressure on agronomic properties of biochar. *Journal of Analytical and Applied Pyrolysis,* 169, 105858. https://doi.org/10.1016/j.jaap.2023.105858

Basinas, P., Rusín, J., Chamrádová, K., & Kaldis, S. P. (2023). Pyrolysis of the anaerobic digestion solid by-product: characterization of digestate decomposition and screening of the biochar use as soil amendment and as additive in anaerobic digestion. *Energy Conversion and Management,* 277, 116658. https://doi.org/10.1016/j.enconman.2023.116658

Binh, Q. A., Nguyen, V. H., & Kajitvichyanukul, P. (2022). Influence of pyrolysis conditions of modified corn cob bio-waste sorbents on adsorption mechanism of atrazine in contaminated water. *Environmental Technology & Innovation*, 26, 102381. https://doi.org/10.1016/j.eti.2022.102381

Boateng, A. A., Garcia-Perez, M., Mašek, O., Brown, R., & del Campo, B. (2015). *Biochar production technology*. In Biochar for environmental management (pp. 63-87). Routledge, London.

Bonanomi, G., Cesarano, G., Iacomino, G., Cozzolino, A., Motti, R., & Idbella, M. (2023). Decomposition of Posidonia oceanica (L.) Delile Leaf Blade and Rhizome in Terrestrial Conditions: Effect of Temperature and Substrate Fertility. *Waste and Biomass Valorization,* 14(6), 1869-1878. https://doi.org/10.1007/s12649-022-01990-9

Brady, N. C., Weil, R. R., & Weil, R. R. (2008). *The nature and properties of soils* (Vol. 13, pp. 662-710). Prentice Hall, Upper Saddle River, NJ.

Bridgwater, A. V. (2012). Review of fast pyrolysis of biomass and product upgrading. *Biomass and bioenergy*, 38, 68-94, https://doi.org/10.1016/j.biombioe.2011.01.048

Carter, S., & Shackley, S. (2011). *Biochar Stoves: an innovation studies perspective.* UK Biochar Research Centre, University of Edinburgh. http://www.build-a-gasifier.com/PDF/BiocharStovesInnovation2011.pdf

Crombie K, Masek O, Sohi SP, Brownsort P, Cross A (2013) The effect of pyrolysis conditions on biochar stability as determined by three methods. *GCB Bioenergy*, 5, 122–131, https://doi.org/10.1111/gcbb.12030

Crombie, K., & Mašek, O. (2015). Pyrolysis biochar systems, balance between bioenergy and carbon sequestration. *Gcb Bioenergy*, 7(2), 349-361, https://doi.org/10.1111/gcbb.12137

Chen, B., Gu, Z., Wu, M., Ma, Z., Lim, H. R., Khoo, K. S., & Show, P. L. (2022). Advancement pathway of biochar resources from macroalgae biomass: A review. *Biomass and Bioenergy*, 167, 106650. https://doi.org/10.1016/j.biombioe.2022.106650

Chen, L., Cheng, P., Ye, L., Chen, H., Xu, X., & Zhu, L. (2020). Biological performance and fouling mitigation in the biochar-amended anaerobic membrane bioreactor (AnMBR) treating pharmaceutical wastewater. *Bioresource technology*, 302, 122805. https://doi.org/10.1016/j.biortech.2020.122805

Chen, W., Gan, L., & Huang, J. (2023). Design, Manufacturing and Functions of Pore-Structured Materials: From Biomimetics to Artificial. *Biomimetics,* 8(2), 140. https://doi.org/10.3390/biomimetics8020140

Chen, Y. X., Huang, X. D., Han, Z. Y., Huang, X., Hu, B., Shi, D. Z., & Wu, W. X. (2010). Effects of bamboo charcoal and bamboo vinegar on nitrogen conservation and heavy metals immobility during pig manure composting. *Chemosphere*, 78(9), 1177-1181, https://doi.org/10.1016/j.chemosphere.2009.12.029

Chen, X., Zhang, J., Lin, Q., Li, G., & Zhao, X. (2023). Dispose of Chinese cabbage waste via hydrothermal carbonization: hydrochar characterization and its potential as a soil amendment. *Environmental Science and Pollution Research*, 30(2), 4592-4602. https://doi.org/10.1007/s11356-022-22359-4

Elkhlifi, Z., Iftikhar, J., Sarraf, M., Ali, B., Saleem, M. H., Ibranshahib, I., ... & Chen, Z. (2023). Potential role of biochar on capturing soil nutrients, carbon sequestration and managing environmental challenges: a review. *Sustainability*, 15(3), 2527. https://doi.org/10.3390/su15032527

Enders A., Hanley K., Whitman T., Joseph S., Lehmann J. (2012) Characterization of biochars to evaluate recalcitrance and agronomic performance. *Bioresource Tech-nology*, 114, 644–653, https://doi.org/10.1016/j.biortech.2012.03.022

Faraji, M., & Saidi, M. (2023). Experimental and simulation study of peanut shell-derived activated carbon and syngas production via integrated pyrolysis-gasification technique. *Process Safety and Environmental Protection*, 171, 874-887. https://doi.org/10.1016/j.psep.2023.01.052

Fatima, B., Bibi, F., Ali, M. I., Woods, J., Ahmad, M., Mubashir, M., ... & Khoo, K. S. (2022). Accompanying effects of sewage sludge and pine needle biochar with selected organic additives on the soil and plant variables. *Waste Management*, 153, 197-208. https://doi.org/10.1016/j.wasman.2022.08.016

Gabhane, J. W., Bhange, V. P., Patil, P. D., Bankar, S. T., & Kumar, S. (2020). Recent trends in biochar production methods and its application as a soil health conditioner: a review. *SN Applied Sciences,* 2, 1-21. https://doi.org/10.1007/s42452-020-3121-5

Guo, S., Li, Y., Wang, Y., Wang, L., Sun, Y., & Liu, L. (2022). Recent advances in biochar-based adsorbents for CO2 capture. *Carbon Capture Science & Technology*, 100059. https://doi.org/10.1016/j.ccst.2022.100059

Grover, P. D., Iyer, P. V. R., & Rao, T. R. (2002). *Biomass thermochemical characterization*, IIT Delhi: MNES, Delhi, India, Third edition.

Hernandez-Mena, L. E., Pécoraa, A. A., & Beraldob, A. L. (2014). Slow pyrolysis of bamboo biomass: analysis of biochar properties. *Chem Eng*, 37, 115-120, https://doi.org/10.3303/CET1437020

Hettithanthri, O., Rajapaksha, A. U., Nanayakkara, N., & Vithanage, M. (2023). Temperature influence on layered double hydroxide tailored corncob biochar and its application for fluoride removal in aqueous media. *Environmental Pollution*, 320, 121054.

Ibitoye, S. E., Mahamood, R. M., Jen, T. C., & Akinlabi, E. T. (2022). Combustion, Physical, and Mechanical Characterization of Composites Fuel Briquettes from Carbonized Banana Stalk and Corncob. *International Journal of Renewable Energy Development*, 11(2). https://doi.org/10.14710/ijred.2022.41290

Idris, S. S., Zailan, M. I., Azron, N., & Rahman, N. A. (2021). Sustainable Green Charcoal Briquette from Food Waste via Microwave Pyrolysis Technique: Influence of Type and Concentration of Binders on Chemical and Physical Characteristics. *International Journal of Renewable Energy Development*, 10(3). https://doi.org/10.14710/ijred.2021.33101

Intagun, W., Khamdaeng, T., Prom-Ngarm, P., & Panyoyai, N. (2018). Effect of core puncture diameter on bio-char kiln efficiency. *International Journal of Biotechnology and Bioengineering*, 12(11), 435-439, https://core.ac.uk/download/pdf/211931141.pdf

Ippolito, J. A., Cui, L., Kammann, C., Wrage-Mönnig, N., Estavillo, J. M., Fuertes-Mendizabal, T., ... & Borchard, N. (2020). Feedstock choice, pyrolysis temperature and type influence biochar characteristics: a comprehensive meta-data analysis review. *Biochar,* 2, 421-438. https://doi.org/10.1007/s42773-020-00067-x

Jeffery, I. E., Akinyemi, O. O., Adedoyin, A. A., & Matthew, U. F. (2023). Potentials of bamboo and its ecological benefits in Nigeria. *Advances in Bamboo Science*, 100032. https://doi.org/10.1016/j.bamboo.2023.100032

Jian, X., Zhuang, X., Li, B., Xu, X., Wei, Z., Song, Y., & Jiang, E. (2018). Comparison of characterization and adsorption of biochars produced from hydrothermal carbonization and pyrolysis. *Environmental Technology & Innovation*, 10, 27-35.

Ji, Y., Zhang, C., Zhang, X. J., Xie, P. F., Wu, C., & Jiang, L. (2022). A high adsorption capacity bamboo biochar for CO2 capture for low temperature heat utilization. *Separation and Purification Technology*, 293, 121131, https://doi.org/10.1016/j.seppur.2022.121131

Kalderis, D., Seifi, A., Trang, T. K., Tsubota, T., Anastopoulos, I., Manariotis, I., ... & Khataee, A. (2023). Bamboo-derived adsorbents for environmental remediation: A review of recent progress. *Environmental Research*, 115533. https://doi.org/10.1016/j.envres.2023.115533

Khaledi, S., Delbari, M., Galavi, H., Bagheri, H., & Chari, M. M. (2023). Effects of biochar particle size, biochar application rate, and moisture content on thermal properties of an unsaturated sandy loam soil. *Soil and Tillage Research*, 226, 105579. https://doi.org/10.1016/j.still.2022.105579

Kumar, S., Rawat, D., Singh, B., & Khanduri, V. P. (2023). Utilization of bamboo resources and their market value in the western Himalayan region of India. *Advances in Bamboo Science*, 100019. https://doi.org/10.1016/j.bamboo.2023.100019

Kurniawan, T. A., Othman, M. H. D., Liang, X., Goh, H. H., Gikas, P., Chong, K. K., & Chew, K. W. (2023). Challenges and opportunities for biochar to promote circular economy and carbon neutrality. *Journal of environmental management*, 332, 117429, https://doi.org/10.1016/j.jenvman.2023.117429

Klüpfel, L., M. Keiluweit, M. Kleber, and M. Sander. 2014. "Redox properties of plant biomass-derived black carbon (biochar)." *Environmental Science & Technology*, 48:5601–5611, https://doi.org/10.1021/es500906d

Kongnine, D. M., Kpelou, P., Attah, N. G., Kombate, S., Mouzou, E., Djeteli, G., & Napo, K. (2020). Energy Resource of Charcoals Derived from Some Tropical Fruits Nuts Shells. *International Journal of Renewable Energy Development,* 9(1). https://doi.org/10.14710/ijred.9.1.29-35

Lee, Y., Park, J., Ryu, C., Gang, K. S., Yang, W., Park, Y. K., ... & Hyun, S. (2013). Comparison of biochar properties from biomass residues produced by slow pyrolysis at 500 C. *Bioresource technology*, 148, 196-201, https://doi.org/10.1016/j.biortech.2013.08.135

Lehmann, J., & Joseph, S. (Eds.). (2015). *Biochar for environmental management: science, technology and implementation*. Routledge, London, https://doi.org/10.4324/9780203762264

Li, L., Long, A., Fossum, B., & Kaiser, M. (2023). Effects of pyrolysis temperature and feedstock type on biochar characteristics pertinent to soil carbon and soil health: A meta-analysis. *Soil Use and Management,* 39(1), 43-52. https://doi.org/10.1111/sum.12848

Liu, Z., Wang, Z., Chen, H., Cai, T., & Liu, Z. (2021). Hydrochar and pyrochar for sorption of pollutants in wastewater and exhaust gas: A critical review. *Environmental Pollution*, 268, 115910. https://doi.org/10.1016/j.envpol.2020.115910

Maneekhat, C., & Khamdaeng, T. (2022). *Thermal Characteristics of Anila-type Biochar Kiln.* Doctoral dissertation, Maejo University, Chiangmai, http://ir.mju.ac.th/dspace/handle/123456789/1237

Meyer, D. (2009*). Biochar - a survey. Special assignment in energy and process engineering*. Finland: Tampere University of Technology.

Mosisa, F. T., Tibba, G. S., & Bayisa, B. (2019). Biochar production using pyrolysis cook stove from coffee husk, wood working wastes and wastes from bedebe brewery. *International Journal of Multidisciplinary Educational Research*, 5(3), 178-187. http://ijmer.s3.amazonaws.com/pdf/volume8/volume8-issue5(3)-2019.pdf#page=187

Muzyka, R., Misztal, E., Hrabak, J., Banks, S. W., & Sajdak, M. (2023). Various biomass pyrolysis conditions influence the porosity and pore size distribution of biochar. *Energy*, 263, 126128. https://doi.org/10.1016/j.energy.2022.126128

Nair, R. R., Kißling, P. A., Marchanka, A., Lecinski, J., Turcios, A. E., Shamsuyeva, M., ... & Weichgrebe, D. (2023). Biochar synthesis from mineral and ash-rich waste biomass, part 2: characterization of biochar and co-pyrolysis mechanism for carbon sequestration. *Sustainable Environment Research*, 33(1), 1-17. https://doi.org/10.1186/s42834-023-00176-9

Ogawa, M., Okimori, Y., & Takahashi, F. (2006). Carbon sequestration by carbonization of biomass and forestation: three case studies. *Mitigation and adaptation strategies for global change*, 11, 429-444, https://doi.org/10.1016/B978-0-12-386505-2.00002-X

Ojolo, S. J., Osheku, C. A., & Sobamowo, M. G. (2013). Analytical Investigations of Kinetic and Heat Transfer in Slow Pyrolysis of a Biomass Particle. *International Journal of Renewable Energy Development*, 2(2), 105-115.

Ong, H. C., Yu, K. L., Chen, W. H., Pillejera, M. K., Bi, X., Tran, K. Q., ... & Petrissans, M. (2021). Variation of lignocellulosic biomass structure from torrefaction: A critical review. *Renewable and Sustainable Energy Reviews*, 152, 111698. https://doi.org/10.1016/j.rser.2021.111698

Onokwai, A. O., Okokpujie, I. P., Ajisegiri, E. S., Oki, M., Adeoye, A. O., & Akinlabi, E. T. (2022). Characterization of Lignocellulosic Biomass Samples in Omu-Aran Metropolis, Kwara State, Nigeria, as Potential Fuel for Pyrolysis Yields. *International Journal of Renewable Energy Development*, 11(4). https://doi.org/10.14710/ijred.2022.45549

Oram, N. J., van de Voorde, T. F., Ouwehand, G. J., Bezemer, T. M., Mommer, L., Jeffery, S., & Van Groenigen, J. W. (2014). Soil amendment with biochar increases the competitive ability of legumes via increased potassium availability. *Agriculture, Ecosystems & Environment*, 191, 92-98, https://doi.org/10.1016/j.agee.2014.03.031

Pradana, Y. S., & Prasetya, A. (2017, March). Performance evaluation of household pyrolytic stove: Effect of outer air holes condition. *In AIP Conference Proceedings* (Vol. 1823, No. 1, p. 020069). *AIP Publishing LLC*, https://doi.org/10.1063/1.4978142

Prakongkep, N., Gilkes, R., Wisawapipat, W., Leksungnoen, P., Kerdchana, C., Inboonchuay, T., ... & Hammecker, C. (2020). Effects of biochar on properties of tropical sandy soils under organic agriculture. *Journal of Agricultural Science*, 13(1), 1-17. https://dx.doi.org/10.5539/jas.v13n1p1

Panyoyai, N., Petchaihan, L., Wongsiriamnuay, T., Hiransatitporn, B., & Khamdaeng, T. (2019). Simulation of temperature distribution in biochar kiln with different feedstock types. *Engineering Access*, 5(2), 59-64, https://ph02.tci-thaijo.org/index.php/mijet/article/download/10.14456.mijet.2019.9/10.14456.mijet.2019.9

Petchaihan, L., Panyoyai, N., Khamdaeng, T., & Wongsiriamnuay, T. (2020, March). Test of a modified small-scale biochar kiln. In *IOP Conference Series: Earth and Environmental Science* (Vol. 463, No. 1, p. 012004). IOP Publishing. https://doi.org/10.1088/1755-1315/463/1/012004

Pinisakul, A., Kruatong, N., Vinitnantharat, S., Wilamas, P., Neamchan, R., Sukkhee, N., ... & Sanghaisuk, S. (2023). Arsenic, Iron, and Manganese Adsorption in Single and Trinary Heavy Metal Solution Systems by Bamboo-Derived Biochars. *C*, 9(2), 40. https://doi.org/10.3390/c9020040

Qian, S., Zhou, X., Fu, Y., Song, B., Yan, H., Chen, Z., ... & Lai, C. (2023). Biochar-compost as a new option for soil improvement: Application in various problem soils. *Science of The Total Environment*, 870, 162024. https://doi.org/10.1016/j.scitotenv.2023.162024

Rusch, F., Wastowski, A. D., de Lira, T. S., Moreira, K. C. C. S. R., & de Moraes Lúcio, D. (2023). Description of the component properties of species of bamboo: a review. *Biomass Conversion and Biorefinery*, 13(3), 2487-2495. https://doi.org/10.1007/s13399-021-01359-3

Rustamaji, H., Prakoso, T., Devianto, H., Widiatmoko, P., Rizkiana, J., & Guan, G. (2022). Synthesis and characterization of hydrochar and bio-oil from hydrothermal carbonization of Sargassum sp. using choline chloride (ChCl) catalyst. *International Journal of Renewable Energy Development*, 11(2)), 403-412. https://doi.org/10.14710/ijred.2022.42595

Sahoo, S. S., Vijay, V. K., Chandra, R., & Kumar, H. (2021). Production and characterization of biochar produced from slow pyrolysis of pigeon pea stalk and bamboo. *Cleaner Engineering and Technology*, 3, 100101, https://doi.org/10.1016/j.clet.2021.100101

Selvarajoo, A., Wong, Y. L., Khoo, K. S., Chen, W. H., & Show, P. L. (2022). Biochar production via pyrolysis of citrus peel fruit waste as a potential usage as solid biofuel. *Chemosphere*, 294, 133671. https://doi.org/10.1016/j.chemosphere.2022.133671

Sayed, E. T., Olabi, A. G., Shehata, N., Al Radi, M., Muhaisen, O. M., Rodriguez, C., ... & Abdelkareem, M. A. (2022). Application of bio-based electrodes in emerging capacitive deionization technology for desalination and wastewater treatment. *Ain Shams Engineering Journal,* 102030. https://doi.org/10.1016/j.asej.2022.102030

Sawarkar, A. D., Shrimankar, D. D., Kumar, A., Kumar, A., Singh, E., Singh, L., ... & Kumar, R. (2020). Commercial clustering of sustainable bamboo species in India. *Industrial Crops and Products,* 154, 112693. https://doi.org/10.1016/j.indcrop.2020.112693

Sawarkar, A. D., Shrimankar, D. D., Kumar, M., Kumar, P., & Singh, L. (2023). Bamboos as a cultivated medicinal grass for industries: A systematic review. *Industrial Crops and Products*, 203, 117210. https://doi.org/10.1016/j.indcrop.2023.117210

Shen, Q., & Wu, H. (2023). Rapid pyrolysis of biochar prepared from slow and fast pyrolysis: the effects of particle residence time on char properties. *Proceedings of the Combustion Institute*, 39(3), 3371-3378. https://doi.org/10.1016/j.proci.2022.07.119

Sittioad, C., Tantikul, S., Wongsiriamnuay, T., Khamdaeng, T., Tippayawong, N., & Panyoyai, N. (2022, November). Temperature distribution and properties of biochar from a two-heating-stage kiln. *In AIP Conference Proceedings* (Vol. 2681, No. 1, p. 020046). AIP Publishing LLC, https://doi.org/10.1063/5.0115161

Smebye, A. B., Sparrevik, M., Schmidt, H. P., & Cornelissen, G. (2017). Life-cycle assessment of biochar production systems in tropical rural areas: Comparing flame curtain kilns to other production methods. *Biomass and Bioenergy,* 101, 35-43. https://doi.org/10.1016/j.biombioe.2017.04.001

Tomczyk, A., Sokołowska, Z., & Boguta, P. (2020). Biochar physicochemical properties: pyrolysis temperature and feedstock kind effects. *Reviews in Environmental Science and Bio/Technology*, 19, 191-215. https://doi.org/10.1007/s11157-020-09523-3

Viglašová, E., Galamboš, M., Danková, Z., Krivosudský, L., Lengauer, C. L., Hood-Nowotny, R., ... & Briančin, J. (2018). Production, characterization and adsorption studies of bamboo-based biochar/montmorillonite composite for nitrate removal. *Waste Management*, 79, 385-394, https://doi.org/10.1016/j.wasman.2018.08.005

Wang, H., Wang, X., Cui, Y., Xue, Z., & Ba, Y. (2018). Slow pyrolysis polygeneration of bamboo (Phyllostachys pubescens): Product yield prediction and biochar formation mechanism. *Bioresource technology*, 263, 444-449, https://doi.org/10.1016/j.biortech.2018.05.040

Wang, L., Xue, C., Nie, X., Liu, Y., & Chen, F. (2018). Effects of biochar application on soil potassium dynamics and crop uptake. *Journal of Plant Nutrition and Soil Science*, 181(5), 635-643, https://doi.org/10.1002/jpln.201700528

Xu, Z., Liu, Y., Chen, H., Yang, M., & Li, H. (2017). Bamboo-like, oxygen-doped carbon tubes with hierarchical pore structure derived from polymer tubes for supercapacitor applications. *Journal of Materials Science*, 52, 7781-7793. https://doi.org/10.1007/s10853-017-1064-z

Yablonovitch, E., & Deckman, H. W. (2023). Scalable, economical, and stable sequestration of agricultural fixed carbon. *Proceedings of the National Academy of Sciences*, 120(16), e2217695120, https://doi.org/10.1073/pnas.2217695120

Yang, K., Yang, J., Jiang, Y., Wu, W., & Lin, D. (2016). Correlations and adsorption mechanisms of aromatic compounds on a high heat temperature treated bamboo biochar. *Environmental Pollution*, 210, 57-64, https://doi.org/10.1016/j.envpol.2015.12.004

You, X., Wang, X., Sun, R., Liu, Q., Fang, S., Kong, Q., ... & Li, Y. (2023). Hydrochar more effectively mitigated nitrous oxide emissions than pyrochar from a coastal soil of the Yellow River Delta, China. *Science of The Total Environment*, 858, 159628. https://doi.org/10.1016/j.scitotenv.2022.159628

Zahida, R., Waseem, R., Kanth, R. H., Ashaq, H., Parmeet, S., Pir, F. A., ... & Aijaz, N. (2017). Biochar: A Tool for Mitigating Climate Change-A Review. *Chem Sci Rev Lett*, 6, 1561-1574. https://chesci.com/wp-content/uploads/2017/08/V6i23_33_CS122048061_Zahida_1561-1574.pdf

Zhang, Y., Chen, F., Chen, D., Cen, K., Zhang, J., & Cao, X. (2020). Upgrading of biomass pellets by torrefaction and its influence on the hydrophobicity, mechanical property, and fuel quality. *Biomass Conversion and Biorefinery,* 1-10. https://doi.org/10.1007/s13399-020-00666-5

Zhao, R., Wang, X., Liu, L., Li, P., & Tian, L. (2019). Slow pyrolysis characteristics of bamboo subfamily evaluated through kinetics and evolved gases analysis. *Bioresource technology*, 289, 121674, https://doi.org/10.1016/j.biortech.2019.121674